HHS Public Access

Author manuscript

Curr Biol. Author manuscript; available in PMC 2024 April 24.

Published in final edited form as:

Curr Biol. 2023 April 24; 33(8): 1613–1623.e5. doi:10.1016/j.cub.2023.03.008.

Chronic sleep loss sensitizes *Drosophila melanogaster* to nitrogen stress

Joseph L. Bedont[1], **Anna Kolesnik**[1], **Pavel Pivarshev**[1], **Dania Malik**[1], **Cynthia T. Hsu**[1], **Aalim Weljie**[1], **Amita Sehgal**[1,2,*]

[1]Chronobiology and Sleep Institute, Perelman School of Medicine, University of Pennsylvania, 3400 Civic Center Boulevard, Philadelphia, PA 19104, United States

[2]Howard Hughes Medical Institute, 4000 Jones Bridge Road, Chevy Chase, MD 20815, United States

Summary

Chronic sleep loss profoundly impacts metabolic health and shortens lifespan, but studies of the mechanisms involved have focused largely on acute sleep deprivation [1,2]. To identify metabolic consequences of chronically reduced sleep, we conducted unbiased metabolomics on heads of three adult *Drosophila* short-sleeping mutants with very different mechanisms of sleep loss: *fumin (fmn)*, *redeye (rye)*, and *sleepless (sss)* [3–7]. Common features included elevated ornithine and polyamines; and lipid, acyl-carnitine, and TCA cycle changes suggesting mitochondrial dysfunction. Studies of excretion demonstrate inefficient nitrogen elimination in adult sleep mutants, likely contributing to their polyamine accumulation. Increasing levels of polyamines, particularly putrescine, promotes sleep in control flies, but poisons sleep mutants. This parallels broadly enhanced toxicity of high dietary nitrogen load from protein in chronically sleep-restricted *Drosophila*, including both sleep mutants and flies with hyper-activated wake-promoting neurons. Together, our results implicate nitrogen stress as a novel mechanism linking chronic sleep loss to adverse health outcomes, and perhaps for linking food and sleep homeostasis at the cellular level in healthy organisms.

eTOC Blurb

Bedont et al. show that fruit fly sleep mutants accumulate polyamines, likely driven by inefficient nitrogen excretion. The authors identify putrescine as a novel somnogen, and find that dietary

*Lead contact: please address inquiries to amita@pennmedicine.upenn.edu.

Author Contributions

JLB and AS conceived the study. JLB, AK, and PP developed and validated methodology as needed, and performed and analyzed most experiments. JLB and AK collected material for all metabolomics studies. DM developed and validated methodology for, and performed and analyzed, our acute sleep loss metabolomics study. CTH developed and validated novel Matlab scripts used for awake time-by-food analysis. JLB, AW, and AS supervised other authors and secured funding for this work. JLB and AS wrote and revised the manuscript. All authors contributed intellectually to this work.

Declaration of Interests

The authors declare no competing interests.

nitrogen is more toxic in chronically sleep deprived flies. This reveals a novel mechanism linking chronic sleep loss to longevity.

Results and Discussion

Sleep mutant, but not acutely sleep deprived, fly heads have remodeled nitrogen metabolism

We conducted metabolomics on ~10-day-old *iso31* control and sleep mutant *fmn*, *rye*, and *sss* fly heads. 30 metabolites were commonly regulated across sleep mutants, which we attribute to chronic sleep loss (Figure 1A). 7 (~23%) of these are primarily linked to nitrogen metabolism or polyamine synthesis: ornithine, acetylarginine, α-acetylornithine, δ-acetylornithine, acetylisoputreanine, diacetylspermidine, and pipecolate (Figure 1B). The polyamines putrescine and spermidine were also elevated in *rye* and *sss*, and putrescine trended high in *fmn* (p=0.0535) (Figure S1A). Other commonly regulated metabolites, such as taurine, sarcosine, and guanine, have links to nitrogen metabolism, but also other pathways (Figure S1B) [8,9].

We then asked if acute sleep deprivation similarly alters nitrogen metabolism. Targeted metabolomics in *iso31* heads at morning zeitgeber time (ZT)2 (control) compared to evening ZT14, ZT2 after overnight sleep deprivation (ZT2 SD), and ZT2 after overnight SD with morning rebound sleep (ZT2 SR), showed minimal effects on nitrogen metabolism. Ornithine alone trended higher at ZT2 SR (Figure S1C). Thus, nitrogen metabolome remodeling in sleep mutants requires chronic sleep loss.

Mitochondrial, lipid, and other metabolome changes in heads of *Drosophila* sleep mutants

5 metabolites commonly regulated across sleep mutants were carnitine or acyl-carnitines, suggesting defects in β-oxidation (Figure 1C). Many other acyl-carnitines were elevated idiosyncratically in particular sleep mutants (Data S1). Elevated 2-methylcitrate and methylmalonate, and lower carboxymethyllysine and aconitate, suggest mitochondrial stress across sleep mutants (Figure 1C) [10–13]. In *rye* and *sss*, mitochondrial defects likely contribute to lipid loss that skews remaining lipid ratios; *fmn* has similar, weaker trends (Figure 1D–E). Cholesteryl esters are also down in *rye* and *sss*, with a similar trend in *fmn* (Data S1). Other commonly regulated metabolites included smaller clusters of threonine and erythrosine derivatives (Figure S1B).

Chronic, but not acute, sleep restriction reduces efficiency of nitrogen excretion

Polyamine synthesis requires considerable nitrogen [9], implying sleep mutants are nitrogen stressed. To test this, we assayed total protein, urate, urea, and NH_4 in ~10-day-old whole flies at dawn and dusk. Urea was unquantifiable, while total protein, NH_4, and urate showed either no effect, or idiosyncratic effects in individual sleep mutants (Figure S2A–F). We next assayed hemolymph total protein and NH_4 in sleep mutant and control flies at dawn and dusk, to assess circulating nitrogen stress. Both were markedly elevated in *rye*; total protein was modestly elevated and NH_4 trended up (p=0.06) in *fmn* (Figure S2G–H). While *sss* lacked these differences (p>0.53), their elevated whole-fly and head urate likely indicates

that they accumulate nitrogen stress in a different form (see Figure S2; Data S1; Discussion). These results encouraged us to examine sleep mutant nitrogen excretion.

Because excretion is an active behavior, we assayed NH_4 and urate excretion at the beginning and end of the day / waking phase, and late at night in ~10-day-old flies. Both metabolites showed a genotype main effect ($p<0.001$), driven by consistently decreased excretion in all sleep mutants, albeit with some mutant-specific variation in time(s) of day driving the effect (Figure 2A–B). To determine whether this reflected constipation, we pre-fed FCF brilliant blue laced food for 24 hours and measured dye excretion (Figure 2C). A genotype main effect ($p<0.0001$) was driven by increased excretion in *rye* and *sss*, across all times for *sss* and mostly in the morning for *rye* (Figure 2C). *fmn* excretion volume was similar to control, but this likely reflects depletion of gut contents during the assay; excrement deposition is increased in *fmn* pre-feeding vials (Figure S2I). Decreased nitrogen metabolites in increased-to-unchanged excrement volume demonstrates inefficient nitrogen excretion in all adult sleep mutants tested.

We next repeated these studies ~1 day after eclosion, when sleep mutants are short-sleeping, but have experienced less lifetime sleep loss [14]. No young sleep mutant had deficient NH_4 or urate excretion, while a genotype main effect on dye excretion ($p<0.0001$) was driven by *decreased* excretion volume in *fmn* and *rye* (Figure 2F). These findings suggest that loss of nitrogen excretion efficiency requires chronic sleep loss.

Lack of an effect on nitrogen excretion might explain the failure of overnight SD to elevate head polyamines, in our study and others (Figure S1) [2]. We tested this by measuring NH_4, urate, and blue dye excretion in ~10 day-old *iso31* flies after 12hr overnight mechanical SD (mechSD) vs unshaken controls. We found increased NH_4 and blue dye and up-trending urate ($p=0.08$) after mechSD (Figure 2G–I). Increased excretion volume suggests that nitrogen excretion efficiency is not necessarily increased by mechSD, but rather that excretion remains largely intact with acute sleep loss.

We next sought to compare excretion after acute and chronic sleep restriction in parallel, independently of sleep-altering mutations. As flies adapt to extended mechanical shaking, we restricted sleep by activating wake-promoting neurons using 60D04-Gal4>TrpA1 (D>Trp) and 11H05-Gal4>TrpA1 (H>Trp) lines. This sleep loss is heat-gated and resists homeostatic rebound, allowing acute and chronic sleep restriction [15,16]. Excretion assays after 1-day and 10-day sleep restriction at 29C were inconclusive, with mostly negative results that may reflect no effect of sleep restriction, perhaps due to lack of sleep need buildup [16], or may instead stem from confounding effects of duration at 29C on excretion in genetic controls (Figure S2J–O). Urate excretion in D>Trp --the one case lacking time-at-29C confounds in genetic controls--was elevated at 1-day 29C but not 10-day 29C, driven by decreased urate excretion only in D>Trp (Figure S2K). This supports our overall results suggesting impairment of nitrogen excretion by chronic sleep restriction.

Blocking terminal polyamine synthesis increases sleep in *Drosophila melanogaster*

Since sleep loss promotes somnogen accumulation, we conducted RNAi screens to test how polyamine metabolism and linked pathways regulate sleep in *Drosophila*. Drug-inducible

geneswitch (GS) drivers allowed adult-specific knockdown. Screening whole fly knockdown with actinGS>dicer yielded hits for argininosuccinate lyase (*asl*), spermidine synthase (*spds*), and spermine synthase (*sms*) (Figures 2J,3A; Data S2). We also screened pan-neuronal knockdown with nsybGS>dicer, but no hits validated (Figure S3A; Data S2). Neither screen recapitulated sleep gain previously reported with constitutive pan-neuronal knockdown of *oat* (Data S2) [17]. Possible explanations include knockdown timing and strain effects.

Our initial experiments used single-beam DAM monitors. Surprisingly, qPCR of actinGS>dicer knockdown of sleep screen hit RNAis (*asl*#1; *spds*#1; *sms*#4) and RNAis lacking sleep screen phenotypes (*asl*#3; *spds*#5; *sms*#5) revealed significant knockdown with all RNAis, with only sleep screen hit *sms*-RNAi#4 appearing to have superior efficacy (Figure S3B). *asl* was comparably decreased by both its RNAis, and *spds*-RNAi#5 appeared *more* effective than screen hit *spds*-RNAi#1 (Figure S3B–H).

Since single-beam confounds can mask sleep-gain phenotypes, we re-tested the four *spds* and *sms* alleles above, and conducted all subsequent sleep experiments, on multi-beam sleep monitors. Adult whole-fly *asl* RNAi#1 decreased total and day sleep, and fragmented sleep (Figure 3B,E; Data S2). Adult whole-fly *spds* RNAi#1 increased total and night sleep, and consolidated sleep, in both sleep assays (Figure 3C,F,H; Data S2). Adult whole-fly *sms* RNAi#4 increased and consolidated sleep, and decreased latency to sleep at ZT12, in both sleep assays (Figure 3D,G,I; Data S2). Consistent with its more robust knockdown, on multi-beam monitors *spds*-RNAi#5 reproduced all sleep phenotypes of *spds*-RNAi#1, increased day sleep, and decreased sleep latency (Figure 3J; Data S2). Consistent with its weaker knockdown, *sms*-RNAi#5 did not replicate most sleep phenotypes of *sms*-RNAi#4 on multi-beam monitors (Figure S3I; Data S2).

Finally, we assayed sleep in actinGS>UAS-cas9.P2 CRISPR knockouts using available *spds* and *asl* sgRNAs. Adult *spds*-KO RU-dependently increased sleep, though without consolidation observed with more-efficient RNAi knockdowns (Figures 3K; S3B,K; Data S2). While activity index (AI), activity per waking minute, was low with actinGS>cas9,spds-sgRNA, low AI was RU-independent (Data S2). Comparable AI decrease, but not total sleep gain, was observed with constitutive actinGal4>cas9,spds-sgRNA (Figures 3K,S3M; Data S2). Thus, like RNAi, *spds* knockout in adulthood increases sleep. While night sleep was RU-dependently fragmented with adult actinGS>cas9,*asl*-sgRNA, total sleep only weakly trended down (Figure S3J; Data S2). However, *asl* transcript also appeared less robustly down-regulated than with RNAi tools, leaving *asl*'s role in sleep unclear (Figure S3B,L). Constitutive actinGal4>cas9,*asl*-sgRNA also did not decrease sleep (Figure S3N).

In sum, even relatively modest loss of *spds* in adulthood increases sleep. Loss of *sms* in adulthood, if near-complete, also increases sleep. And our data are inconclusive on whether *asl* loss in adulthood decreases sleep. Together, our data show that blocking terminal polyamine synthesis (i.e: putrescine conversion into spermidine or spermine) is sleep promoting (Figure 2J).

Putrescine promotes sleep in control flies, but polyamines are toxic to sleep mutants

We next tested sleep in *iso31* flies on food laced with vehicle or 16mM L-ornithine, putrescine, or spermidine. Putrescine increased total sleep, driven primarily by increased and consolidated day sleep, with decreased ZT0 latency to sleep (Figures 3L–O; S3O–R; Data S2). Females may also sleep more at night with shortened ZT12 latency on putrescine, though a small decrease in night AI leaves unclear whether this reflects nocturnal lethargy (Figure S3P; Data S2). Regardless, most female and all male sleep gain came from day sleep, and neither sex has decreased day AI ($p>0.8$) (Data S2). Together, this indicates putrescine is a novel somnogen.

This view is reinforced by weak, day-sleep promoting effects of spermidine and ornithine, which can convert to putrescine either directly (from ornithine) or via acetylated intermediates (Figure 2J). Spermidine increased day sleep in males and decreased ZT0 sleep latency in both sexes, with no AI changes (Figures 3L–O; S3O–R; Data S2). Surprisingly, 16mM ornithine did not affect sleep in either sex (Figures 3L–O; S3O–R; Data S2) [17]. Re-testing at the maximal 50mM dose previously reported, in females we replicated shorter ZT0 sleep latency, but observed only a modest uptrend in total sleep ($p=0.0579$), driven by increased and consolidated day sleep with no day AI change (Figures 3P–Q; S3S–V; Data S2). Together, we observe much weaker, but directionally consistent, effects of ornithine on mated female sleep than previously reported [17]. Position confounds on single-beam monitors may partially explain the weaker phenotype; we observe dose-dependent chemo-repulsion on ornithine, driving increased time spent by females at the tube midpoint at 16mM (Figure S3W–Z). Strain differences may also contribute.

Strong sleep-promoting effects of putrescine; weaker, sexually dimorphic sleep-promoting effects of spermidine and high-dose ornithine; and sleep-promoting effects of adult *spds* and *sms* knockdown, all point to putrescine as the primary polyamine somnogen (Figure 2J). This model also accommodates other results, including possible sleep-decrease with adult *asl* knockdown, and previously reported sleep gain with constitutive neuronal *oat* knockdown [17].

We next tested whether polyamines could rescue sleep in sleep mutants. However, this proved impossible—sleep mutants were markedly locomotor impaired and rapidly killed by 16mM polyamine food. This prompted us to conduct an acute 6-day survival study of sleep mutant and control flies on single-beam sleep monitors, comparing within-genotype toxicity on our sleep-study metabolites. Spermidine reduced survival (Surv) only in *fmn* and *sss* females, and putrescine decreased survival severely in female sleep mutants, but only modestly in *iso31* (Figure 4A–D). In males, putrescine reduced survival in all three sleep mutants but not *iso31*, while spermidine reduced survival only in *sss* (Figure 4E–H). Ornithine had no effect (Figure 4A–H). Polyamine effects on hazard ratio (HR) mirrored survival.

Chronic sleep restriction renders flies sensitive to dietary nitrogen

Polyamine toxicity is consistent with dietary nitrogen sensitivity. Indeed, in previous reports *fmn* flies had normal lifespan on standard food, but short lifespan on nitrogen-rich, high-

calorie diet [4,18]. However, *sss* (and chronic short-sleep generally) are associated with short lifespan [1,6,15]. In our hands, all three sleep mutants (including *fmn*) have short lifespan on standard food (Figure S4A–B) [4]. Thus, general ill-health might explain sleep mutant sensitivity to polyamines. To assess specific sensitivity to nitrogen stress, we tested *iso31* and sleep mutant lifespan on: (1) high-protein, (2) high-sugar, and (3) all-sugar diets. In wild-type *Drosophila*, nitrogen rich high-protein and nitrogen starvation all-sugar diets both shorten lifespan, relative to high-sugar diet with low protein [19,20].

While all-sugar narrowed survival differences between sleep mutants and *iso31*, sleep mutants remained short-lived on all three diets (Figure S4C–H). However, within-genotype diet comparisons suggested nitrogen sensitivity of sleep mutants. In *iso31*, lifespan and hazard was generally high-sugar > high-protein > all-sugar (Figure 4I,M). Sleep mutants performed better on all-sugar vs high-protein, with (1) a narrowed “penalty” on all-sugar in *fmn*; (2) no lifespan and blunted hazard differences in *rye*; and (3) longer lifespan/lower hazard on all-sugar in *sss* (Figure 4I–P). The lifespan/hazard “penalty” on all-sugar vs high-sugar was also blunted or lost across sleep mutants, especially males (Figure 4I–P). However, high-protein vs high-sugar effects varied (Figure 4I–P).

Differential feeding could impact lifespan directly, and protein both promotes postprandial sleep and reduces sleep depth, which could impact sleep restriction [21–23]. To test whether either factor contributes to our complex lifespan results, we simultaneously measured awake time-by-food and sleep on multibeam sleep monitors (Data S3). This approach avoids climbing proficiency and aversive shock confounds inherent to alternative methods, such as Café and FLIC assays [24], though chemotaxis is a potential confound. Sleep mutants spend more awake time near food than *iso31* on all diets, suggesting that overfeeding may contribute to their diet-independent, baseline lifespan reduction (Figure S4A–J). Importantly, diet-independent overfeeding is consistent with increased excretion volume from adult sleep mutants (Figures 2C,S2I), corroborating that awake time-by-food grossly tracks feeding behavior in our flies. Sleep mutants are short-sleeping on all diets, and presumptive overfeeding is driven primarily by increased awake time (Data S3).

We next compared within-genotype awake time-by-food on different diets. *iso31* dwelled at high-protein > high-sugar > all-sugar. *rye* and *sss* also dwelled at high protein > both other diets, while *fmn* dwelled similarly at all diets (Figure S4I). Thus, *rye* and *sss* mutants with less “*iso*-like” diet effects on lifespan had more “*iso*-like” diet effects on presumptive feeding time, while *fmn* had the most “*iso*-like” effects of diet on lifespan and the least “*iso*-like” effects of diet on presumptive feeding time (Figures 4I–P;S4I). This misalignment suggests that feeding differences do not account for differential effects of diet on longevity of sleep mutants vs *iso31*.

iso31 also slept less on high-protein and high-sugar vs all-sugar; *fmn* slept equivalently on all 3 diets, *rye* slept more on high-protein vs all-sugar, and *sss* slept more on high-protein vs both other diets (Data S3). Diet-induced sleep increases generally do not coincide with AI decreases (Data S3). Relative sleep gains in sleep mutants from dietary nitrogen are unlikely to enhance nitrogen toxicity, and may mitigate it, contributing to our sleep mutant longevity results’ complexity.

Genotype-specific metabolic differences in sleep mutants, including uricotelic pathways that couple sugar intake to nitrogen metabolism, may also contribute to this complexity (Figures 1–2,S1–S2; Data S1) [25]. To side-step this, we next tested lifespan on the same diets at 29C in chronically sleep-restricted D>Trp and H>Trp flies. In DGal4, HGal4, and TrpA1 genetic controls, lifespan on high-sugar > high-protein > all-sugar, much like *iso31* at 25C (Figure 4Q,R,T,V,W,Y). In contrast, D>Trp flies, while longest-lived on high-sugar, had equivalent lifespan and hazard on high-protein and all-sugar (Figure 4S,X). H>Trp flies showed even more robust effects; both sexes lived longer on all-sugar than high-protein, and males had comparable lifespan and hazard on all-sugar vs high-sugar (Figure 4U,Z). All-sugar diet also rescued lifespan and hazard compared to one or both genetic controls in D>Trp males and all H>Trp flies (Figure S4J–U). These results are consistent with enhanced toxicity of dietary nitrogen, and reduced toxicity or outright protective effects of nitrogen starvation, during chronic sleep loss.

These results are also not attributable to feeding or sleep. Gal4 control, D>Trp, and H>Trp groups all spent awake time at high-protein > high-sugar > all-sugar; TrpA1 controls dwelled similarly at all-sugar and high-protein, but TrpA1 lifespan on high-protein was > all-sugar, like Gal4 controls (Figure S4V–W). Like sleep mutants, D>Trp and H>Trp sleep-restricted flies dwelled longer at all diets vs control genotypes, suggesting that fasting does not drive all-sugar rescue of sleep-restricted lifespan and hazard (Figure S4J–W). D>Trp and H>Trp flies were also sleep-restricted at 29C on all diets, with no within-genotype diet effects on total sleep (Data S3).

Discussion

In this study, we sought metabolic changes common across sleep mutants as candidate effectors of chronic sleep loss on health. Lipid and mitochondrial dysregulation likely contribute to sleep mutant ill health, given redox factors that link sleep to lifespan [15,26]. But lipid-metabolism is also widely reported to be affected by acute SD across species [2,27–31]. High methylcitrate and low aconitate after acute SD have also been reported, as have effects of lipid metabolism on sleep [27,32–34]. Thus, we pursued our findings of altered nitrogen metabolism.

Consistent with reports of its elevation during or after acute SD [35,36], ornithine alone trended up during recovery sleep after mechSD (Figure S1) and may be a leading indicator of nitrogen stress during acute sleep loss. To our knowledge, our finding that polyamines accumulate in sleep mutant heads is the first report of this chronic sleep loss effect in the tissues of any organism [2]. However, indirect evidence suggests this extends to humans. Sleep apnea patients excrete elevated ornithine and polyamines [37,38]; we found no similar reports with acute SD [2]. And acute SD increases putrescine in hyperammonemic but not control rat brain dialysate, consistent with accumulated nitrogen stress being required for polyamine elevation [39].

Terrestrial insects generally lack Otc for urea cycling, and excrete mostly uricotelic metabolites and raw NH_4, suggesting sleep mutants with inefficient nitrogen excretion should be hyperammonemic [8] (Figure 2J).Consistent with this, hemolymph total protein and

NH_4 tend to be high in adult *fmn* and *rye*, but puzzlingly not *sss* (Figure S2G–H). This likely reflects a a P-element in the *sss* mutant that provides the only functional *white* cassette in our sleep mutant studies; a *white* homolog regulates urate metabolism in silkworm [40]. Accordingly, *sss* alone among our sleep mutant and *iso31* control genotypes has very high urate (Figure S2C,F; Data S1), which causes nitrogen stress in excess [41]. Thus, all three sleep mutants build up nitrogen stress in some form. Polyamine accumulation may buffer this, soaking up nitrogen equivalents, which would reduce but not eliminate nitrogen stress. In fact, polyamines switch from protective to themselves driving nitrogen stress in excess, especially putrescine and acetylated polyamines most enriched in sleep mutant heads (Figures 1,S1) [9].

A role of sleep in nitrogen homeostasis may explain the putrescine soporific function demonstrated by our supplementation and RNAi studies (Figures.2J,3,S3). Polyamine levels are fine-tuned in cells due to their myriad critical roles, including in sleep-relevant pathways like redox balance and autophagy [1,9,15,26,42]. Homeostasis is achieved by elaborate and well-conserved synthetic, trafficking, and degradation mechanisms [9]. Putrescine's somnogenic role may complement these cellular mechanisms, dialing up sleep to help bring polyamine levels down if systemic putrescine rises too high. Sleep remains low in short-sleeping mutants despite high polyamines because homeostatic effectors are impaired.

Finally, we report a novel interaction between chronic sleep loss and diet that regulates longevity (Figure 4). High-protein and all-sugar toxicity relative to high-sugar is well known for wild-type flies [19,20]. We show that sleep-restricted flies live longer on all-sugar than high-protein compared to control flies, suggesting sensitivity to dietary nitrogen (Figures 2J;4). This was particularly prominent with thermogenetic sleep loss in D>Gal4 and H>Gal4 flies, which showed outright protective effects of all-sugar diet (Figure S4). Sleep-restricted males also appeared somewhat more nitrogen-sensitive than females, perhaps because egg-laying offloads nitrogen.

Our findings have several implications for health. Pathologically, redox balance couples sleep loss to lifespan [15,26]. Nitrogen stress is oxidizing, with even generally anti-oxidant species like polyamines and urate becoming oxidizing in excess [9,41]. Likely, nitrogen stress drives a subset of metabolic onramps converging on systemic oxidation and short lifespan during chronic sleep loss. Nitrogen stress may also be relevant for sleep loss associated disease. Kidney disease is associated with chronic sleep loss in humans [43,44], and elevated putrescine and polyamine degradation products contribute to kidney failure [45]. Chronic sleep loss is also associated with Alzheimer's disease [46]; animal models suggest nitrogen stress precedes cognitive decline [47] and drives beta-amyloid pathology via polyamine synthesis [48], while human Alzheimer's brains compensate by remodeling nitrogen metabolism away from polyamine synthesis [48,49].

Finally, our work has teleological implications for behavior observed in healthy humans, like increasing sugar intake when sleep-restricted [50,51]. Going for the cookies instead of protein-rich food when tired may constitute surprisingly adaptive interactions of the food and sleep homeostasis systems, avoiding nitrogen intake during a period of heightened sensitivity.

STAR Methods

RESOURCE AVAILABILITY

Lead Contact—Requests for further information, resources, or reagents should be directed to Prof. Amita Sehgal at amita@pennmedicine.upenn.edu.

Materials Availability—This study entirely used previously published and/or publically available fly lines.

Data and Code Availability—Our HD4 global metabolomics dataset is deposited on Metabolights at https://www.ebi.ac.uk/metabolights/MTBLS3318.

Previously unreported scripts for time-at-position (multibeamPositionAnalysis_minutesPerDay.m) and awake time-at-position analysis (posWhileAwakeToExcel.m) were deposited to the repository on GitHub (https://github.com/cthsu86/damSleepConverter). Other code used has been previously reported [52].

Other data and additional information required to reanalyze data reported in this paper is available from the lead contact upon request.

EXPERIMENTAL MODEL DETAILS: *Drosophila melanogaster*

Heavily used fly lines in the manuscript include *iso31* control; sleep mutants *fmn*, *rye*, and *sss* on an *iso31* background (minimum 5X generations); and geneswitch/dicer lines that were well-established in the lab prior to this study [42]. RNAi and sgRNA alleles were ordered from Bloomington Drosophila Stock Center in Indiana, Vienna Drosophila Resource Center in Austria, or Kyoto Stock Center in Japan. UAS-Cas9.P2 (II) was ordered from Bloomington and crossed to our existing ActinGS and ActinGal4 (III) alleles. 60D04- and 11H05-gal4 lines were generously gifted by Kyunghee Koh, and crossed to our existing uas-trpA1 (II) line for thermogenetic studies. See Data S2 for details of each RNAi and sgRNA line used in the manuscript. Except where otherwise noted, adult flies were raised in 12:12LD light:dark cycle incubators at ~25C and ~65% humidity. Mated flies were used for all studies, with the exception of Figure 2D–F, many of which were likely virginal given their youth at the time of collection. Sex and age varied by experiment, as specified in our METHOD DETAILS (next) and figure legends.

METHOD DETAILS

Metabolon global metabolomics and lipidomics—Ten total pools of ~200–250 heads from mixed sex flies aged ~1–2 weeks post-eclosion (~10 days on average) were collected for each genotype, split evenly between HD4 global metabolomics and CLP lipidomics assays. Sexes were pooled to mitigate the large numbers required for the study. Collections were done at ~ZT6; mid-day timepoint was chosen to enrich for metabolites dysregulated by chronic, as opposed to acute, sleep loss. Heads were collected by vortexing whole flies snap frozen on dry ice and separating heads from bodies by size on dry ice-cooled grates. Samples were stored at −80C and shipped to Metabolon on dry ice. Sample

preparation, control procedures, and analysis were carried out at Metabolon Inc as described elsewhere [53–57]. Both HD4 and CLP procedures are briefly outlined below.

HD4 Global Metabolomics—Samples extracted and spiked with recovery standards using a MicroSTAR System (Hamilton Company) and methanol-precipitated under vigorous shaking Genogrinder 2000 (Glen Mills). Samples were fractionated, dried, resuspended in appropriate solvents, and analyzed using four distinct modes on a Waters ACQUITY ultra-performance liquid chromatography (UPLC) and a Thermo Scientific Q-Exactive high resolution/accurate mass spectrometer interfaced with a heated electrospray ionization (HESI-II) source and Orbitrap mass analyzer operated at 35,000 mass resolution. Metabolites were identified by the Laboratory Information Management System, an automated system that identified ion features in our head lysate samples using a reference library of known metabolites defined by retention time, molecular weight (m/z), preferred adducts, in-source fragments, and associated MS spectra. The data was curated by visual quality control using software developed at Metabolon. Raw data for each metabolite was scaled to its internal median, after imputing the smallest non-zero value for that metabolite for any zeroes.

CLP Lipidomics—Lipids were extracted using a modified Bligh-Dyer extraction method with deuterated internal standards. Samples were then subjected to infusion-MS analysis in both positive and negative modes on a Shimadzu LC with nano PEEK tubing and a Sciex SelexIon-5500 QTRAP in MRM mode (>1,100 MRMs). Individual lipids were quantified as signal / internal standard and summed into class and total lipid concentrations.

Acute SD targeted nitrogen metabolomics—Twenty total pools of ~90 mixed sex *iso31* flies aged ~1.5 weeks post-eclosion were divided evenly among four conditions: (1) collected at ZT2, (2) collected at ZT14, (3) collected at ZT2 after a 14hr mechanical sleep deprivation, and (4) collected at ZT2 after a 12hr sleep deprivation followed by a 2hr sleep rebound. Heads were collected by vortexing whole flies snap frozen on dry ice and separating heads from bodies by size on dry ice-cooled grates. Samples were stored at −80C until they were processed. Samples were extracted and prepared for LC-MS analysis as previously described [58,59]. Briefly, a stainless steel bead and 300 µl of 2:1 Methanol:Chloroform were added to each sample. Samples were homogenized for a total of 4 minutes at 25 Hz in a tissue homogenizer. Next, 100 µl of water and chloroform were added to each sample. Samples were vortexed and then centrifuged for 10 minutes at 13,300 rpm at 4°C. 170 µl of the upper fraction containing polar metabolites was collected from each sample and dried in a speed vacuum for 2.5 hours. Dried fractions were resuspended in 100 µl of acetonitrile:water, vortexed for 20 seconds and centrifuged for 10 minutes at 13,300 rpm at 4°C prior to transferring to MS vials. Samples were analyzed in analytical triplicates and pooled quality control samples were run at the beginning and end of the run as well as after every 6th injection. For each sample, 2 µl were injected onto an Acquity UPLC BEH Amide column (1.7 µm, 2.1 mm × 150 mm) with a 0.2 µm inline precolumn filter using an Acquity H-Class UPLC system (Waters Corporation) coupled to a Xevo TQ-S micro mass spectrometer operating in a positive ion polarity mode. Initial chromatographic conditions consisted of 100% Solvent

D (90:10 Acetonitrile:water, 2 mM Ammonium Acetate, 0.2% Formic Acid) ramped to 79.4% Solvent A (95:5 milliQH2O:Acetontrile, 2 mM Ammonium Acetate, 0.2% Formic Acid) in 15 minutes. The column was washed in 100% Solvent A for 5.5 minutes before reequilibrating in 100% D. A total of 18 compounds were measured through targeted MRM methods. Transitions for Urea, Sarcosine, Proline, Trans-4-Hydroxyproline, Ornithine, Spermidine, Acetylornithine, Citrulline, SAM, Spermine, Glutamate, 4-Guanidinobutanoic Acid, Creatine, Acetylputrescine, and GABA were used as described in [59]. Additional transitions were added for Argininosuccinate (291.13/70.07 (15/40) [(Cone Voltage/ Collision Energy]), Arginine (157.14/60.05 (30/12)), and Putrescine (88.9/54.86 (14/16) and 89.11/72.08 (15/20)). Data was processed using TargetLynx (Waters) to obtain ion counts for further analysis using an in-house R-script. Spermine is excluded from our results because of low signal / high noise that rendered the signal suspect. Urea is excluded from our results because we were unable to corroborate its relevance through biochemical methods.

Lysate collection from whole flies for biochemistry—Whole bodies were used in lieu of heads because of difficulty consistently detecting many target metabolites in heads using biochemical methods. Pools of 5 female or 5 male ~10-day post-eclosion flies were anesthetized with CO2 and quickly sorted into 2mL Safelock Tubes, weighed, then snap frozen on dry ice. Blocks were pre-chilled to 4C, and the tubes were transferred to wet ice, where 200uL of 1X PBS supplemented with 1 cOmplete EDTA-free protease inhibitor tablet / 2.5mLs PBS (PBS-PI) and a stainless steel bead were added. Samples were quickly loaded into chilled blocks and lysed on a TissueLyser II (Qiagen) at 25.0m/sec in two 2-min bursts. Beads were removed and solid detritus was pelleted by spinning at 15,000rpm for 15min at 4C. Supernatant was carefully transferred to a clean tube and diluted 1:4 in PBS-PI before being used for total protein, ammonia, and urate (uric acid) biochemical assays.

Hemolymph collection from female flies for biochemistry—Only female flies were run for these experiments because their typical hemolymph volume is much higher than males. Groups of 25 ~10-day post-eclosion flies were anesthetized with CO_2, rapidly pricked in the thorax with tungsten probes (Ted Pella 13570), and loaded into 0.5mL Ependorfs perforated at the base with 22-gauge syringe tips, which were nested inside of 1.5mL Ependorfs containing 45uL of PBS-PI. Nested tubes were then centrifuged at 5000rpm for 5min at 4C. 25uL of hemolymph + PBS-PI was removed for total protein analysis, and the remaining ~20uL was diluted with a further 60uL of PBS-PI for ammonia analysis. Flies were weighed after hemolymph harvest.

Excrement collection from male flies for biochemistry—Only male flies were run for these experiments to eliminate egg-laying as a confound. Groups of 12 flies were anesthetized with CO2 and sorted into 1.5mL Ependorf tubes perforated twice through each cap with an 18-gauge needle. The flies were returned to their home incubators for 2 hours, then anesthetized with CO2 and flipped into fresh 1.5mL Ependorf tubes to be weighed. The excrement in the first set of Ependorfs was resuspended by vortexing into 150uL of PBS-PI, which was used at this concentration to run ammonia and urate (uric acid) biochemical assays. For sleep mutant studies, ~10 day or ~1 day post-eclosion flies were tested at ZT0-2, ZT10-12, or ZT17-19. For acute mechanical SD studies, ~10 day post-eclosion flies were

sleep deprived for 12hr overnight and tested at ZT0-2. For thermogenetic SD studies, ~1–4 day post-eclosion flies raised in an 18–20C room were (i) stored at 18C for ~9 days, then moved to 29C for ~1 day of acute sleep restriction before testing, or (ii) stored at 29C for ~10 days of chronic sleep restriction before testing. Thermogenetic flies were entrained to 12:12LD during the ~10 day variable temperature period, and excretion was tested at 29C from ZT10-12 (zeitgeber time chosen for most consistent excretion effects in sleep mutants).

Biochemical Assays: Total Protein, Ammonia, Uric Acid, Urea—Total protein assay was conducted using an Abcam 207003 total protein assay kit according to manufacturer instructions: absorbance measured at 540nm. Ammonia assay was conducted using a Sigma-Aldrich MAK310 kit according to manufacturer instructions: fluorescence measured at excitation 355nm / emission 460nm. Uric acid assay was conducted using a Sigma-Aldrich MAK077 kit according to manufacturer instructions: fluorescence measured at excitation 535nm / emission 595nm. Signal from all biochemical assays was normalized to body weight of the pools of flies that provided the material. Fluorescence and absorbance were measured using a Victor-3V plate reader (Perkin-Elmer) or a Cytation 5 (BioTek).

Blue-Poo Assay—Male flies were pre-fed on our lab's standard yeast-molasses food supplemented with 2.5mg/mL of FD&C blue 1 / FCF brilliant blue dye for 24 hours. Excrement was then collected and resuspended into 150uL of MilliQ water. Absorbance was measured at 620nm and normalized to body weight to calculate fecal volume.

Sleep Experiments—For polyamine supplementation experiments, ~3–5 days post-eclosion flies of both sexes were loaded into locomotor tubes with 5% sucrose / 2% agar food supplemented with water vehicle, 16mM L-ornithine monohydrochloride (Sigma-Aldrich 2375), 16mM putrescine dihydrochloride (Sigma-Aldrich P7505), or 16mM spermidine trihydrochloride (Sigma-Aldrich S2501). Sleep was measured from movements on DAM5H multibeam monitors (Trikinetics), averaged across the 2^{nd}-4^{th} full days of recording. A follow-up study with vehicle vs 50mM L-ornithine monohydrochloride was later conducted separately. Supplement doses were chosen based on a pilot dosing curve assaying sleep and toxicity with DAM2 monitors (data not shown) and published work supporting 16mM as a reasonable dose for screening sleep effects with amino acids and chemically similar polyamines [17,60]. In addition to standard sleep and activity metrics, average time spent / day at each of the 15 possible beam positions is reported for these datasets.

For nitrogen metabolism RNAi screen, ~3–5 days post-eclosion female flies were loaded into locomotor tubes with 5% sucrose / 2% agar food supplemented with 500uM mifepristone (RU+ food) (Sigma-Aldrich M8046). Only females were used for this screen and all follow-up behavior and qPCR experiments, because lower female baseline sleep allows more reliable detection of sleep gain phenotypes, especially with the relatively small n's used for behavioral screening. Sleep was recorded from counts of beam breaks on single-beam DAM2 monitors (Trikinetics), and the 4^{th}-5^{th} full days of exposure to RU+ food were averaged to determine sleep. Geneswitch(GS)>Dicer,RNAi crosses with mean sleep at least 60 min higher or lower than both GS>Dicer and RNAi controls were considered potential hits and validated. Validation of promising crosses was carried out similarly to

the screen, but included both RU+ and ethanol vehicle (RU-) food conditions to assess whether effects were acute. If the first validation experiment was inconsistent with the initial screen result for a given RNAi, further validation of that RNAi was terminated. At least two independent validation experiments were run for each nitrogen RNAi cross identified as having a legitimate sleep phenotype. Hits showing sleep gain were subsequently re-validated by analyzing movements collected on DAM5H multibeam sleep monitors, to rule out possible position confounds. Later follow-up RNAi and Crispr studies were setup similarly to the description above, but used DAM5H multibeam monitors from the outset.

For awake-time-by-food and sleep analysis of sleep mutant and thermogenetic sleep-restriction flies and their genotypic controls, only male flies were used to avoid oviposition as a confound. ~3–5 days post-eclosion males were loaded onto DAM5H multibeam sleep monitors in locomotor tubes containing high-protein, high-sugar, or all-sugar diets used for lifespan analysis (below). Movements and position distribution were recorded from full Days 2–4 post-loading, averaged, and used to calculate standard sleep and activity metrics, as well as absolute and % awake time / day spent adjacent to food.

DAMfilescan and previously reportedcustom MatLab scripts were used to calculate sleep metrics for both sets of experiments [52]. Awake time-by-sleep scripts are novel, and archived at GitHub (see above).

qPCR Validation of Nitrogen Pathway RNAis—To confirm knockdown of target transcripts with RNAi and Crispr tools, we drove expression with actinGS>dcr (RNAi) or actinGS>cas9 (Crispr) and followed the same whole-fly RNA collection, cDNA synthesis, and qPCR method we published previously [42]. The following qPCR primer sets were used for each target transcript: *asl* forward: TCGACAAGCTGTCCCAAGTG reverse: CACCAGATAGTAGGCCCAGTC *spds* forward: GAAACACGCGCTGAAGGATG reverse: GGCATAGGCCACCTTAGCAA *sms* forward: GAGCTGCAGAACATTGCTGA reverse: GTACAACAAGGCGCCATCAC *α-tubulin* forward: CGTCTGGACCACAAGTTCGA reverse: CCTCCATACCCTCACCAACGT

Lifespan Experiments—For all lifespan studies, mated flies of both sexes that had eclosed within the preceding ~2 days (sleep mutant studies) or ~3–4 days (thermogenetic studies) were collected under CO2 anesthesia and housed single-sex on standard or special food at a maximum density of 30/vial.

For classical lifespan studies, flies were flipped to fresh vials and dead were tallied every 3 days (experiments comparing sleep mutant lifespans to control on standard food) or every 2 days (all other experiments). Lifespan vials were co-housed in their incubators with water dishes, to provide supplemental humidity. The w/v of nourishing solutes of roughly similar caloric density were equal for each diet, to minimize differences in caloric density among the diets. Each vial was longitudinally maintained on the same assigned food condition, and dead flies were counted at each flip, tracking survival in this way until all flies were dead. Flies were never again anesthetized after initial collection. Flies that escaped during flips were excluded from analysis.

Sehgal Lab Standard Yeast-Molasses Diet: 64.7g/L corn meal; 27.1g/L dry yeast; 8g/L agar; 61.6mL/L molasses; 10.2mL/L 20% tegosept; 2.5mL/L propionic acid

High-Protein Diet: Sehgal Lab Standard Yeast-Molasses + extra 116g/L yeast

High-Sugar Diet: Sehgal Lab Standard Yeast-Molasses + extra 116g/L sucrose

All-Sugar Diet: 27% w/v sucrose-agar with 10.2mL/L 20% tegosept and 2.5ml/L propionic acid.

For survival on nitrogenous metabolite supplementation studies, flies were initially maintained on standard food, then loaded into locomotor tubes containing 5% sucrose / 2% agar food drugged with either water vehicle or 16mM ornithine, putrescine, or spermidine at ~3–4 days post-eclosion. Behavior was recorded using single-beam DAM monitors until the end of the sixth complete day on supplemented food. Sleep records were analyzed similarly to starvation-challenge, except that all flies surviving past the sixth full day of recording were censored.

QUANTIFICATION AND STATISTICAL ANALYSIS

For molecular studies where lower n's precluded reliable normality pre-testing, a parametric distribution was assumed. For sleep and feeding behavior experiments, higher n's allowed reliable Shapiro-Wilkes pre-testing of all groups' normality to determine whether parametric or non-parametric testing was appropriate for each metric, in each individual experiment. Lifespan studies used specialized non-parametric and semi-parametric statistical approaches. Prism or JMP software was used to carry out all statistical analyses. The following tests were used in the indicated conditions:

--Two groups, or multiple control groups vs one experimental group [61]: Welch's t-test (parametric) or Mann-Whitney test (non-parametric).

--Single control group vs multiple experimental groups: Dunnett test (parametric) or Steel test (non-parametric). Where multiple Dunnett tests were required, they were run as posthoc tests of a two-way ANOVA model.

--All-to-all comparisons, or complex subsets of all comparisons: Tukey HSD test (parametric) or Steel-Dwass test (non-parametric)

--% awake time near food (Data S3) is reported as raw percentages for more intuitive presentation of the data, but statistical tests were conducted on arcsin-transformed percentage values, to more closely approximate an unbounded distribution.

--Mass spectrometry: Welch's t-tests with Benjamini-Hochberg FDR correction.

--qPCR validation of RNAi knockdown efficiency: one-tailed t-tests

--Lifespan: Wilcoxon tests were used to measure differences in survival. Likelihood tests of differences in Cox proportional hazard ratios were used to measure differences in hazard.

Posthoc Bonferroni correction was applied to the significance threshold for survival and hazard comparisons where familywise error was cumulative [62].

Additional details for individual experiments (n definition and number, summary statistics, etc) can be found in corresponding Figure Legends.

Supplementary Material

Refer to Web version on PubMed Central for supplementary material.

Acknowledgements

The Howard Hughes Medical Institute, R01DK120757, NIA F32 AG056081, and NINDS K99 NS118561 funded this work.

References

1. Mignot E (2008). Why We Sleep: The Temporal Organization of Recovery. PLoS Biol 6, e106. 10.1371/journal.pbio.0060106. [PubMed: 18447584]
2. Malik DM, Paschos GK, Sehgal A, and Weljie AM (2020). Circadian and Sleep Metabolomics Across Species. Journal of Molecular Biology 432, 3578–3610. 10.1016/j.jmb.2020.04.027. [PubMed: 32376454]
3. Dubowy C, and Sehgal A (2017). Circadian Rhythms and Sleep in *Drosophila melanogaster*. Genetics 205, 1373–1397. 10.1534/genetics.115.185157. [PubMed: 28360128]
4. Kume K, Kume S, Park SK, Hirsh J, and Jackson FR (2005). Dopamine is a regulator of arousal in the fruit fly. J. Neurosci. 25, 7377–7384. 10.1523/JNEUROSCI.2048-05.2005. [PubMed: 16093388]
5. Shi M, Yue Z, Kuryatov A, Lindstrom JM, and Sehgal A (2014). Identification of Redeye, a new sleep-regulating protein whose expression is modulated by sleep amount. Elife 3, e01473. 10.7554/eLife.01473. [PubMed: 24497543]
6. Koh K, Joiner WJ, Wu MN, Yue Z, Smith CJ, and Sehgal A (2008). Identification of SLEEPLESS, a sleep-promoting factor. Science 321, 372–376. 10.1126/science.1155942. [PubMed: 18635795]
7. Chen W-F, Maguire S, Sowcik M, Luo W, Koh K, and Sehgal A (2015). A neuron-glia interaction involving GABA transaminase contributes to sleep loss in sleepless mutants. Mol. Psychiatry 20, 240–251. 10.1038/mp.2014.11. [PubMed: 24637426]
8. Weihrauch D, and O'Donnell MJ (2021). Mechanisms of nitrogen excretion in insects. Current Opinion in Insect Science 47, 25–30. 10.1016/j.cois.2021.02.007. [PubMed: 33609767]
9. Miller-Fleming L, Olin-Sandoval V, Campbell K, and Ralser M (2015). Remaining Mysteries of Molecular Biology: The Role of Polyamines in the Cell. Journal of Molecular Biology 427, 3389–3406. 10.1016/j.jmb.2015.06.020. [PubMed: 26156863]
10. Yan L-J, Levine RL, and Sohal RS (1997). Oxidative damage during aging targets mitochondrial aconitase. Proceedings of the National Academy of Sciences 94, 11168–11172. 10.1073/pnas.94.21.11168.
11. Fu M-X, Requena JR, Jenkins AJ, Lyons TJ, Baynes JW, and Thorpe SR (1996). The Advanced Glycation End Product, Nϵ-(Carboxymethyl)lysine, Is a Product of both Lipid Peroxidation and Glycoxidation Reactions. Journal of Biological Chemistry 271, 9982–9986. 10.1074/jbc.271.17.9982. [PubMed: 8626637]
12. Amaral AU, Cecatto C, Castilho RF, and Wajner M (2016). 2-Methylcitric acid impairs glutamate metabolism and induces permeability transition in brain mitochondria. J Neurochem 137, 62–75. 10.1111/jnc.13544. [PubMed: 26800654]
13. Melo DR, Mirandola SR, Assunção NA, and Castilho RF (2012). Methylmalonate impairs mitochondrial respiration supported by NADH-linked substrates: Involvement of mitochondrial glutamate metabolism. J. Neurosci. Res. 90, 1190–1199. 10.1002/jnr.23020. [PubMed: 22488725]

14. Dilley LC, Vigderman A, Williams CE, and Kayser MS (2018). Behavioral and genetic features of sleep ontogeny in Drosophila. Sleep 41. 10.1093/sleep/zsy086.

15. Vaccaro A, Kaplan Dor Y, Nambara K, Pollina EA, Lin C, Greenberg ME, and Rogulja D (2020). Sleep Loss Can Cause Death through Accumulation of Reactive Oxygen Species in the Gut. Cell 181, 1307–1328.e15. 10.1016/j.cell.2020.04.049. [PubMed: 32502393]

16. Seidner G, Robinson JE, Wu M, Worden K, Masek P, Roberts SW, Keene AC, and Joiner WJ (2015). Identification of Neurons with a Privileged Role in Sleep Homeostasis in Drosophila melanogaster. Curr Biol 25, 2928–2938. 10.1016/j.cub.2015.10.006. [PubMed: 26526372]

17. Kanaya HJ, Park S, Kim J, Kusumi J, Krenenou S, Sawatari E, Sato A, Lee J, Bang H, Kobayakawa Y, et al. (2020). A sleep-like state in *Hydra* unravels conserved sleep mechanisms during the evolutionary development of the central nervous system. Sci. Adv. 6, eabb9415. 10.1126/sciadv.abb9415. [PubMed: 33028524]

18. Yamazaki M, Tomita J, Takahama K, Ueno T, Mitsuyoshi M, Sakamoto E, Kume S, and Kume K (2012). High calorie diet augments age-associats sleep impairment in Drosophila. Biochemical and Biophysical Research Communications 417, 812–816. 10.1016/j.bbrc.2011.12.041. [PubMed: 22197809]

19. Fontana L, Partridge L, and Longo VD (2010). Extending healthy life span--from yeast to humans. Science 328, 321–326. 10.1126/science.1172539. [PubMed: 20395504]

20. Good TP, and Tatar M (2001). Age-specific mortality and reproduction respond to adult dietary restriction in Drosophila melanogaster. J Insect Physiol 47, 1467–1473. 10.1016/s0022-1910(01)00138-x. [PubMed: 12770153]

21. Longo VD, and Panda S (2016). Fasting, Circadian Rhythms, and Time-Restricted Feeding in Healthy Lifespan. Cell Metab 23, 1048–1059. 10.1016/j.cmet.2016.06.001. [PubMed: 27304506]

22. Murphy KR, Deshpande SA, Yurgel ME, Quinn JP, Weissbach JL, Keene AC, Dawson-Scully K, Huber R, Tomchik SM, and Ja WW (2016). Postprandial sleep mechanics in Drosophila. Elife 5, e19334. 10.7554/eLife.19334. [PubMed: 27873574]

23. Brown EB, Shah KD, Faville R, Kottler B, and Keene AC (2020). Drosophila insulin-like peptide 2 mediates dietary regulation of sleep intensity. PLoS Genet 16, e1008270. 10.1371/journal.pgen.1008270. [PubMed: 32160200]

24. Mishra P, Yang SE, Montgomery AB, Reed AR, Rodan AR, and Rothenfluh A (2021). The fly liquid-food electroshock assay (FLEA) suggests opposite roles for neuropeptide F in avoidance of bitterness and shock. BMC Biol 19, 31. 10.1186/s12915-021-00969-7. [PubMed: 33593351]

25. van Dam E, van Leeuwen LAG, Dos Santos E, James J, Best L, Lennicke C, Vincent AJ, Marinos G, Foley A, Buricova M, et al. (2020). Sugar-Induced Obesity and Insulin Resistance Are Uncoupled from Shortened Survival in Drosophila. Cell Metab 31, 710–725.e7. 10.1016/j.cmet.2020.02.016. [PubMed: 32197072]

26. Hill VM, O'Connor RM, Sissoko GB, Irobunda IS, Leong S, Canman JC, Stavropoulos N, and Shirasu-Hiza M (2018). A bidirectional relationship between sleep and oxidative stress in Drosophila. PLoS Biol. 16, e2005206. 10.1371/journal.pbio.2005206. [PubMed: 30001323]

27. Thimgan MS, Seugnet L, Turk J, and Shaw PJ (2015). Identification of genes associated with resilience/vulnerability to sleep deprivation and starvation in Drosophila. Sleep 38, 801–814. 10.5665/sleep.4680. [PubMed: 25409104]

28. Cirelli C, Gutierrez CM, and Tononi G (2004). Extensive and Divergent Effects of Sleep and Wakefulness on Brain Gene Expression. Neuron 41, 35–43. 10.1016/S0896-6273(03)00814-6. [PubMed: 14715133]

29. Weljie AM, Meerlo P, Goel N, Sengupta A, Kayser MS, Abel T, Birnbaum MJ, Dinges DF, and Sehgal A (2015). Oxalic acid and diacylglycerol 36:3 are cross-species markers of sleep debt. Proc. Natl. Acad. Sci. U.S.A. 112, 2569–2574. 10.1073/pnas.1417432112. [PubMed: 25675494]

30. Davies SK, Ang JE, Revell VL, Holmes B, Mann A, Robertson FP, Cui N, Middleton B, Ackermann K, Kayser M, et al. (2014). Effect of sleep deprivation on the human metabolome. Proceedings of the National Academy of Sciences 111, 10761–10766. 10.1073/pnas.1402663111.

31. Hinard V, Mikhail C, Pradervand S, Curie T, Houtkooper RH, Auwerx J, Franken P, and Tafti M (2012). Key Electrophysiological, Molecular, and Metabolic Signatures of Sleep and

Wakefulness Revealed in Primary Cortical Cultures. Journal of Neuroscience 32, 12506–12517. 10.1523/JNEUROSCI.2306-12.2012. [PubMed: 22956841]

32. Pamboro ELS, Brown EB, and Keene AC (2020). Dietary fatty acids promote sleep through a taste-independent mechanism. Genes, Brain and Behavior 19. 10.1111/gbb.12629.
33. Thimgan MS, Suzuki Y, Seugnet L, Gottschalk L, and Shaw PJ (2010). The perilipin homologue, lipid storage droplet 2, regulates sleep homeostasis and prevents learning impairments following sleep loss. PLoS Biol. 8. 10.1371/journal.pbio.1000466.
34. Thimgan MS, Kress N, Lisse J, Fiebelman C, and Hilderbrand T (2018). The acyl-CoA Synthetase, pudgy, Promotes Sleep and Is Required for the Homeostatic Response to Sleep Deprivation. Front. Endocrinol. 9, 464. 10.3389/fendo.2018.00464.
35. Grant LK, Ftouni S, Nijagal B, De Souza DP, Tull D, McConville MJ, Rajaratnam SMW, Lockley SW, and Anderson C (2019). Circadian and wake-dependent changes in human plasma polar metabolites during prolonged wakefulness: A preliminary analysis. Sci Rep 9, 4428. 10.1038/s41598-019-40353-8. [PubMed: 30872634]
36. Honma A, Revell VL, Gunn PJ, Davies SK, Middleton B, Raynaud FI, and Skene DJ (2020). Effect of acute total sleep deprivation on plasma melatonin, cortisol and metabolite rhythms in females. Eur J Neurosci 51, 366–378. 10.1111/ejn.14411. [PubMed: 30929284]
37. Xu H, Zheng X, Qian Y, Guan J, Yi H, Zou J, Wang Y, Meng L, Zhao A, Yin S, et al. (2016). Metabolomics Profiling for Obstructive Sleep Apnea and Simple Snorers. Sci Rep 6, 30958. 10.1038/srep30958. [PubMed: 27480913]
38. Xu H, Li X, Zheng X, Xia Y, Fu Y, Li X, Qian Y, Zou J, Zhao A, Guan J, et al. (2018). Pediatric Obstructive Sleep Apnea is Associated With Changes in the Oral Microbiome and Urinary Metabolomics Profile: A Pilot Study. Journal of Clinical Sleep Medicine 14, 1559–1567. 10.5664/jcsm.7336. [PubMed: 30176961]
39. Marini S, Santangeli O, Saarelainen P, Middleton B, Chowdhury N, Skene DJ, Costa R, Porkka-Heiskanen T, and Montagnese S (2017). Abnormalities in the Polysomnographic, Adenosine and Metabolic Response to Sleep Deprivation in an Animal Model of Hyperammonemia. Front Physiol 8, 636. 10.3389/fphys.2017.00636. [PubMed: 28912724]
40. Wang L, Kiuchi T, Fujii T, Daimon T, Li M, Banno Y, Kikuta S, Kikawada T, Katsuma S, and Shimada T (2013). Mutation of a novel ABC transporter gene is responsible for the failure to incorporate uric acid in the epidermis of ok mutants of the silkworm, Bombyx mori. Insect Biochem Mol Biol 43, 562–571. 10.1016/j.ibmb.2013.03.011. [PubMed: 23567590]
41. Sautin YY, and Johnson RJ (2008). Uric acid: the oxidant-antioxidant paradox. Nucleosides Nucleotides Nucleic Acids 27, 608–619. 10.1080/15257770802138558. [PubMed: 18600514]
42. Bedont JL, Toda H, Shi M, Park CH, Quake C, Stein C, Kolesnik A, and Sehgal A (2021). Short and long sleeping mutants reveal links between sleep and macroautophagy. eLife 10, e64140. 10.7554/eLife.64140. [PubMed: 34085929]
43. Chen J, Ricardo AC, Reid KJ, Lash J, Chung J, Patel SR, Daviglus ML, Huang T, Liu L, Hernandez R, et al. (2022). Sleep, cardiovascular risk factors, and kidney function: The Multi-Ethnic Study of Atherosclerosis (MESA). Sleep Health, S2352–7218(22)00144–9. 10.1016/j.sleh.2022.08.004.
44. Yin S, Wang J, Bai Y, Yang Z, Cui J, and Wang J (2022). Association between sleep duration and kidney stones in 34 190 American adults: A cross-sectional analysis of NHANES 2007–2018. Sleep Health, S2352721822001425. 10.1016/j.sleh.2022.08.003.
45. Igarashi K, Ueda S, Yoshida K, and Kashiwagi K (2006). Polyamines in renal failure. Amino Acids 31, 477–483. 10.1007/s00726-006-0264-7. [PubMed: 16554974]
46. Winer JR, and Mander BA (2018). Waking Up to the Importance of Sleep in the Pathogenesis of Alzheimer Disease. JAMA Neurol 75, 654. 10.1001/jamaneurol.2018.0005. [PubMed: 29532083]
47. Bergin DH, Jing Y, Mockett BG, Zhang H, Abraham WC, and Liu P (2018). Altered plasma arginine metabolome precedes behavioural and brain arginine metabolomic profile changes in the APPswe/PS1ΔE9 mouse model of Alzheimer's disease. Transl Psychiatry 8, 108. 10.1038/s41398-018-0149-z. [PubMed: 29802260]
48. Ju YH, Bhalla M, Hyeon SJ, Oh JE, Yoo S, Chae U, Kwon J, Koh W, Lim J, Park YM, et al. (2022). Astrocytic urea cycle detoxifies Aβ-derived ammonia while impairing memory

in Alzheimer's disease. Cell Metab 34, 1104–1120.e8. 10.1016/j.cmet.2022.05.011. [PubMed: 35738259]

49. Bensemain F, Hot D, Ferreira S, Dumont J, Bombois S, Maurage C-A, Huot L, Hermant X, Levillain E, Hubans C, et al. (2009). Evidence for induction of the ornithine transcarbamylase expression in Alzheimer's disease. Mol. Psychiatry 14, 106–116. 10.1038/sj.mp.4002089. [PubMed: 17893704]
50. Spiegel K, Tasali E, Penev P, and Cauter EV (2004). Brief Communication: Sleep Curtailment in Healthy Young Men Is Associated with Decreased Leptin Levels, Elevated Ghrelin Levels, and Increased Hunger and Appetite. Ann Intern Med 141, 846. 10.7326/0003-4819-141-11-200412070-00008. [PubMed: 15583226]
51. Bhutani S, Howard JD, Reynolds R, Zee PC, Gottfried J, and Kahnt T (2019). Olfactory connectivity mediates sleep-dependent food choices in humans. eLife 8, e49053. 10.7554/eLife.49053. [PubMed: 31591965]
52. Hsu CT, Choi JTY, and Sehgal A (2020). Manipulations of the olfactory circuit highlight the role of sensory stimulation in regulating sleep amount. Sleep, zsaa265. 10.1093/sleep/zsaa265.
53. Nieman DC, Gillitt ND, Sha W, Esposito D, and Ramamoorthy S (2018). Metabolic recovery from heavy exertion following banana compared to sugar beverage or water only ingestion: A randomized, crossover trial. PLoS ONE 13, e0194843. 10.1371/journal.pone.0194843. [PubMed: 29566095]
54. Kuang A, Erlund I, Herder C, Westerhuis JA, Tuomilehto J, and Cornelis MC (2018). Lipidomic Response to Coffee Consumption. Nutrients 10, E1851. 10.3390/nu10121851.
55. Ubhi BK (2018). Direct Infusion-Tandem Mass Spectrometry (DI-MS/MS) Analysis of Complex Lipids in Human Plasma and Serum Using the Lipidyzer™ Platform. In Clinical Metabolomics Methods in Molecular Biology, Giera M, ed. (Springer New York), pp. 227–236. 10.1007/978-1-4939-7592-1_15.
56. Lintonen TPI, Baker PRS, Suoniemi M, Ubhi BK, Koistinen KM, Duchoslav E, Campbell JL, and Ekroos K (2014). Differential Mobility Spectrometry-Driven Shotgun Lipidomics. Anal. Chem. 86, 9662–9669. 10.1021/ac5021744. [PubMed: 25160652]
57. Baker PRS, Armando AM, Campbell JL, Quehenberger O, and Dennis EA (2014). Three-dimensional enhanced lipidomics analysis combining UPLC, differential ion mobility spectrometry, and mass spectrometric separation strategies. Journal of Lipid Research 55, 2432–2442. 10.1194/jlr.D051581. [PubMed: 25225680]
58. Rhoades SD, and Weljie AM (2016). Comprehensive Optimization of LC-MS Metabolomics Methods Using Design of Experiments (COLMeD). Metabolomics 12, 183. 10.1007/s11306-016-1132-4. [PubMed: 28348510]
59. Malik DM, Rhoades S, and Weljie A (2018). Extraction and Analysis of Pan-metabolome Polar Metabolites by Ultra Performance Liquid Chromatography-Tandem Mass Spectrometry (UPLC-MS/MS). Bio Protoc 8, e2715. 10.21769/BioProtoc.2715.
60. Ki Y, and Lim C (2019). Sleep-promoting effects of threonine link amino acid metabolism in Drosophila neuron to GABAergic control of sleep drive. eLife 8, e40593. 10.7554/eLife.40593. [PubMed: 31313987]
61. Shaffer JP (1995). Multiple Hypothesis Testing. Annu. Rev. Psychol. 46, 561–584. 10.1146/annurev.ps.46.020195.003021.
62. Logan BR, Wang H, and Zhang M-J (2005). Pairwise multiple comparison adjustment in survival analysis. Stat Med 24, 2509–2523. 10.1002/sim.2125. [PubMed: 15977296]
63. Ryder E, Blows F, Ashburner M, Bautista-Llacer R, Coulson D, Drummond J, Webster J, Gubb D, Gunton N, Johnson G, et al. (2004). The DrosDel Collection: A Set of *P*-Element Insertions for Generating Custom Chromosomal Aberrations in *Drosophila melanogaster*. Genetics 167, 797–813. 10.1534/genetics.104.026658. [PubMed: 15238529]
64. Jenett A, Rubin GM, Ngo T-TB, Shepherd D, Murphy C, Dionne H, Pfeiffer BD, Cavallaro A, Hall D, Jeter J, et al. (2012). A GAL4-Driver Line Resource for Drosophila Neurobiology. Cell Reports 2, 991–1001. 10.1016/j.celrep.2012.09.011. [PubMed: 23063364]

65. Hamada FN, Rosenzweig M, Kang K, Pulver SR, Ghezzi A, Jegla TJ, and Garrity PA (2008). An internal thermal sensor controlling temperature preference in Drosophila. Nature 454, 217–220. 10.1038/nature07001. [PubMed: 18548007]

66. Rogulja D, and Irvine KD (2005). Regulation of cell proliferation by a morphogen gradient. Cell 123, 449–461. 10.1016/j.cell.2005.08.030. [PubMed: 16269336]

67. Bai L, Lee Y, Hsu CT, Williams JA, Cavanaugh D, Zheng X, Stein C, Haynes P, Wang H, Gutmann DH, et al. (2018). A Conserved Circadian Function for the Neurofibromatosis 1 Gene. Cell Rep 22, 3416–3426. 10.1016/j.celrep.2018.03.014 [PubMed: 29590612]

Highlights

- Nitrogen metabolism is remodeled in sleep mutants, but not after acute sleep loss.
- Nitrogen excretion efficiency is impaired by chronic, but not acute, sleep loss.
- Polyamines, primarily putrescine, are novel somnogens.
- Chronic sleep loss exacerbates the toxicity of dietary nitrogen sources.

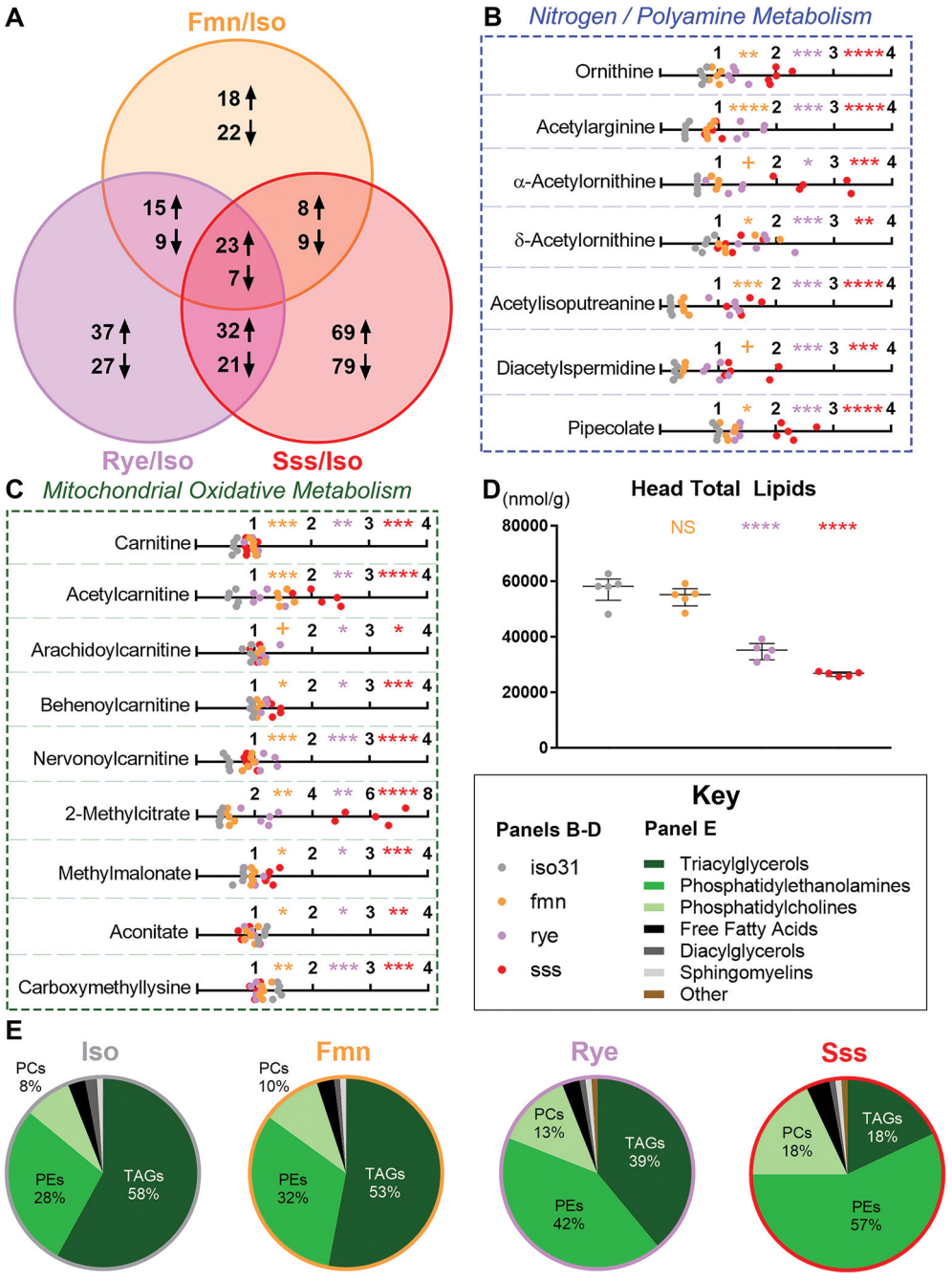

Figure 1. Sleep mutants have profoundly altered nitrogen, mitochondrial, and lipid metabolism.

All metabolomic data is from *iso31* (gray), *fmn* (orange), *rye* (purple), and *sss* (red) pools of ~10-day-old, mixed-sex, mated fly heads collected at ~ZT6. All statistical comparisons shown are color-matched sleep mutant vs *iso31* control.

(A) Venn diagram of the number of metabolites consistently up- or down-regulated in one or more sleep mutants compared to *iso31* control.

(B-C) Line graphs of scaled metabolite levels, grouped by involvement in nitrogen metabolism (B) or mitochondrial oxidative metabolism (C). Data shown are individual pools

of lysate; n=5; Welch's t-tests (p-values) with FDR correction for multiple comparisons (q-values); + p<0.05 but q>0.05, * p/q<0.05, ** p/q<0.01, *** p/q<0.001, **** p/q<0.0001. **(D)** XY graph of total lipid content. Data shown are individual pools of lysate overlaid with median+/−interquartiles; n=5; Dunnett test; NS = not significant, ****p<0.0001. **(E)** Pie graphs showing % of major lipid families in the head lipidome. Changes in sleep mutant lipid composition are largely driven by lost lipids (D), mostly triacylglycerols, especially in *rye* and *sss*.

Related to Figure S1 and Data S1.

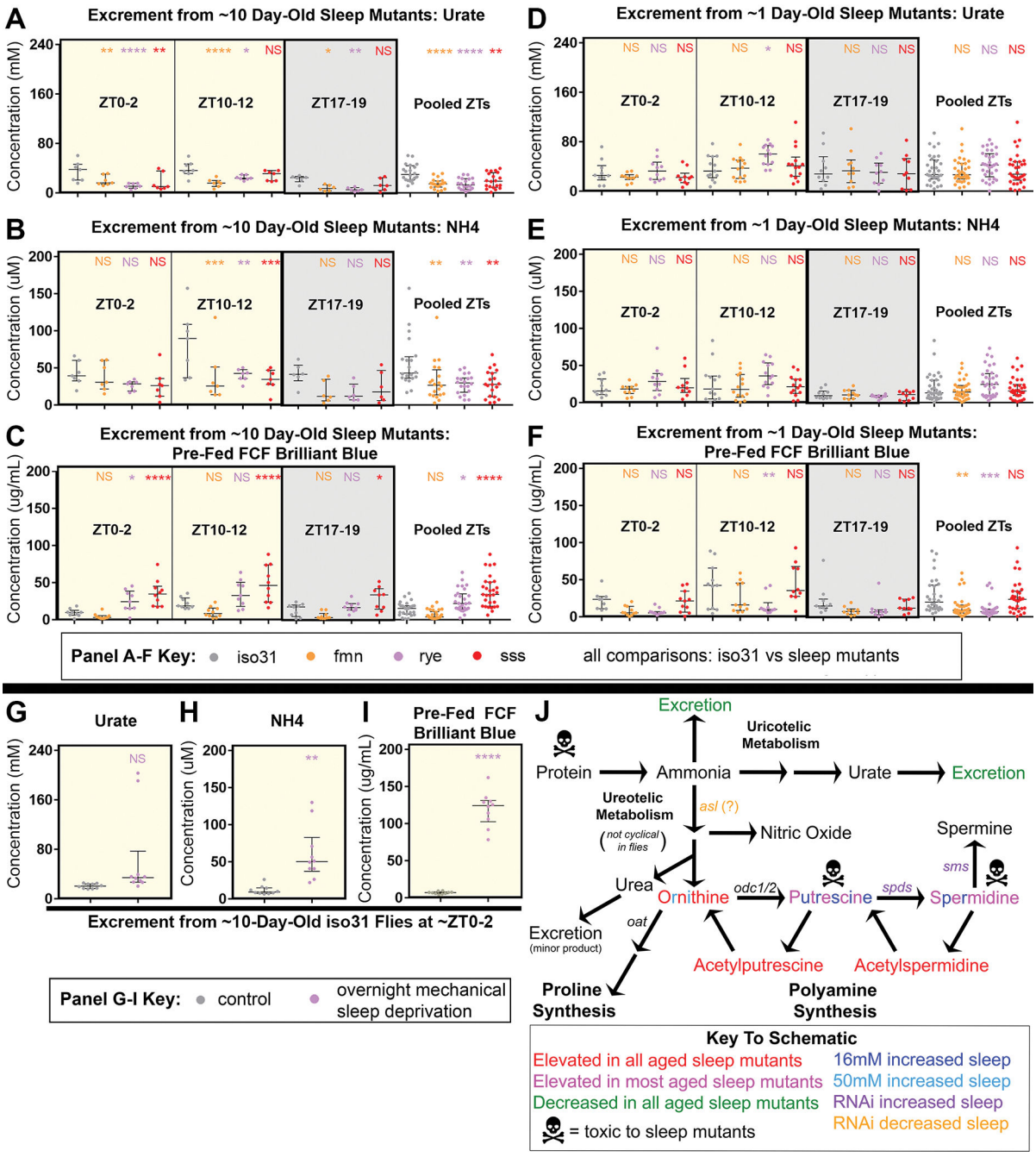

Figure 2. Adult sleep mutants, but not newly eclosed sleep mutants or acutely mechanical sleep deprived adults, inefficiently excrete nitrogen waste.

All data are from male flies at the indicated zeitgeber time (ZT). ~10-day-old flies were mated; mating status of ~1-day-old flies was mixed. All statistical comparisons shown are for color-matched sleep mutant or mechanical SD vs control.

(A-F) Excreted urate (A,D), NH_4 (B,E), and FCF brilliant blue pre-fed for 1 day before collection (C,F) at ZT0-2, ZT10-12, or ZT17-19 from *iso31* (gray), *fmn* (orange), *rye* (purple), and *sss* (red) flies. Flies were ~10 days (A-C) or ~1 day (D-F) old post-eclosion.

n=6–7 per group (10-day-old) or n=10–14 per group (1-day-old); two-way ANOVA with within-ZT and pooled post-hoc Dunnett tests.

(G-I) Excreted urate (G), NH_4 (H), and FCF brilliant blue pre-fed for 1 day before collection (I) at ZT0-2 from control unshaken (gray) or overnight 12-hour mechanically sleep-deprived (purple) *iso31* flies. n=10; Welch tests.

All data shown are from resuspended excretions collected over the indicated 2-hour span from individual pools of flies, overlaid with median+/−interquartiles. NS = not significant, * p<0.05, ** p<0.01, *** p<0.001, **** p<0.0001.

(J) Schematic of ureotelic and uricotelic nitrogen metabolism pathways in *Drosophila melanogaster*. Metabolite levels in sleep mutants and their excretions are in Figures 1–2. Effects of polyamine manipulations on sleep are in Figure 3. Effects of polyamines and protein on lifespan are in Figure 4.

Related to Figure S2.

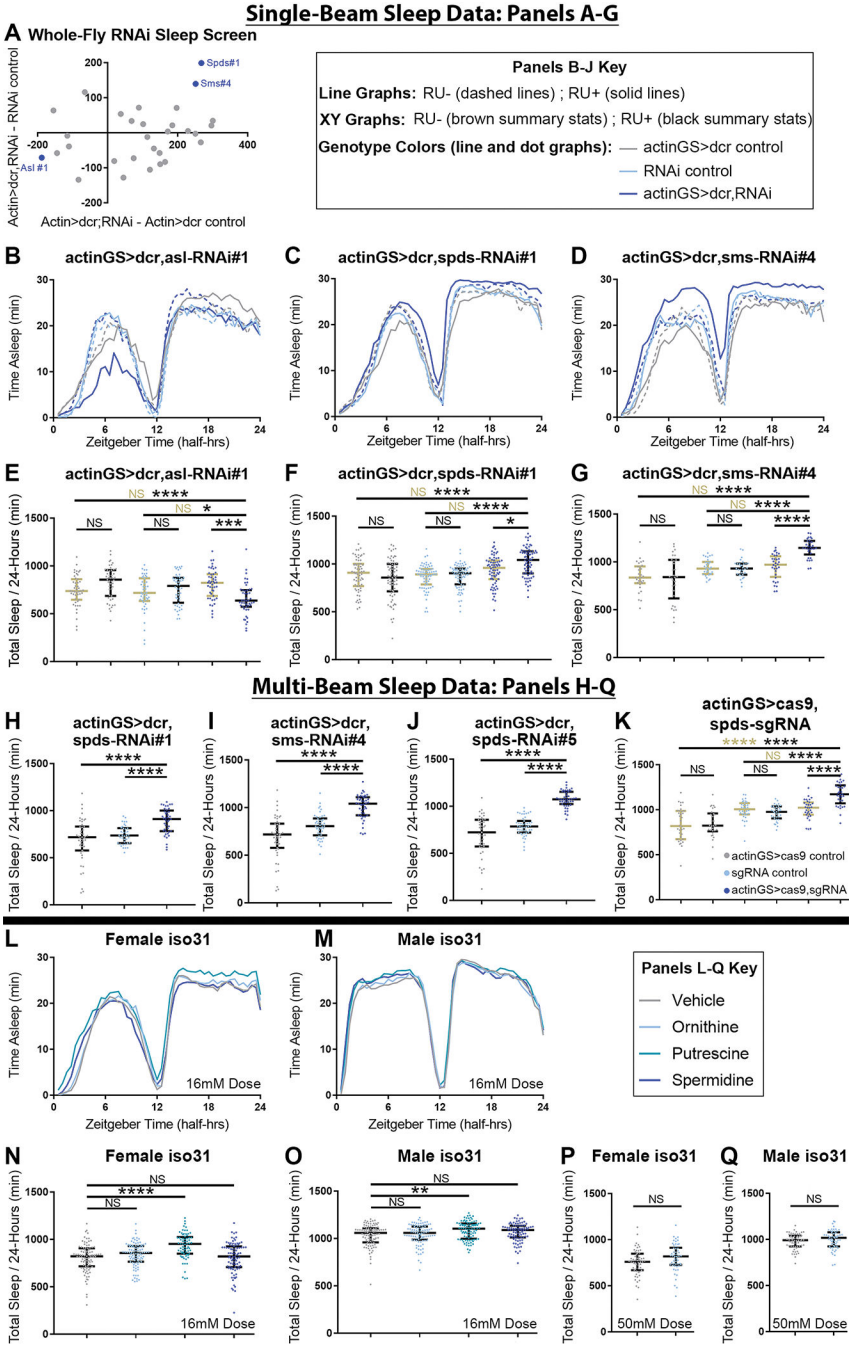

Figure 3. Sleep is increased by both supplementing putrescine and blocking its conversion to terminal polyamines.

All data was collected from adult mated flies.

(A) Difference in single-beam first-pass population mean sleep on mifepristone-laced (RU+) food for various female actin-geneswitch(GS)>dicer;nitrogen metabolism-RNAi crosses, compared with actinGS>dicer control (x-axis) and RNAi control (y-axis). Blue, labeled dots indicate significant hits that passed all validation steps. RNAi identities and population statistics for the screens are provided in Data S2.

(B-G) Sleep data from single-beam validation experiments of screen hits. Whole-fly knockdown of argininosuccinate lyase (*asl*,B,E) RU-dependently decreased sleep. Whole-fly knockdown of spermidine synthase (*spds*,C,F) and spermine synthase (*sms,D,G*) RU-dependently increased sleep. n=30–71 flies per group; Tukey HSD (G) or Steel-Dwass (E,F) tests; statistics for genotype comparisons are color-coded for vehicle control (RU-, brown) or RU+ (black) food.

(H-J) Multi-beam sleep data was collected on RU+ food, to further validate *spds* and *sms* RNAi sleep gain hits with whole-fly knockdown (H-I) and to re-test another *spds* RNAi that qPCR results suggested should increase sleep (J). All increased sleep. n=38–47; Welch's t-tests.

(K) Multi-beam sleep data on vehicle control or RU+ food, from actinGS>cas9,spds-sgRNA experimental flies with actinGS>cas9 and *spds*-sgRNA alone controls. Like RNAi, adult Crispr knockout of *spds* increased sleep. n=30–35; Tukey HSD.

(L-M) Averaged multi-beam sleep behavior of *iso31* females (G) or males (H) plotted over circadian time, on food supplemented with water vehicle (gray), 16mM L-ornithine (light blue), 16mM putrescine (turquoise), or 16mM spermidine (dark blue).

(N-O) Multi-beam total sleep in female (N) and male (O) flies on 16mM or vehicle supplemented food. n=69–93 flies per group; Steel tests (vs Vehicle).

(P-Q) Multi-beam total sleep in female (P) and male (Q) flies on 50mM ornithine (light blue) or vehicle (gray) supplemented food. n=54–58; Welch's t-tests.

The same datasets were used to compute panels shown here and corresponding auxiliary sleep and activity metrics in Figure S3 and Data S2.

For Panels B-Q, all line graphs show averaged sleep behavior over time, and all dot graphs show individual fly values overlaid with median+/−interquartiles. For all panels, NS = not significant, * $p<0.05$; ** $p<0.01$; ***$p<0.001$; **** $p<0.0001$.

Related to Figure S3 and Data S2.

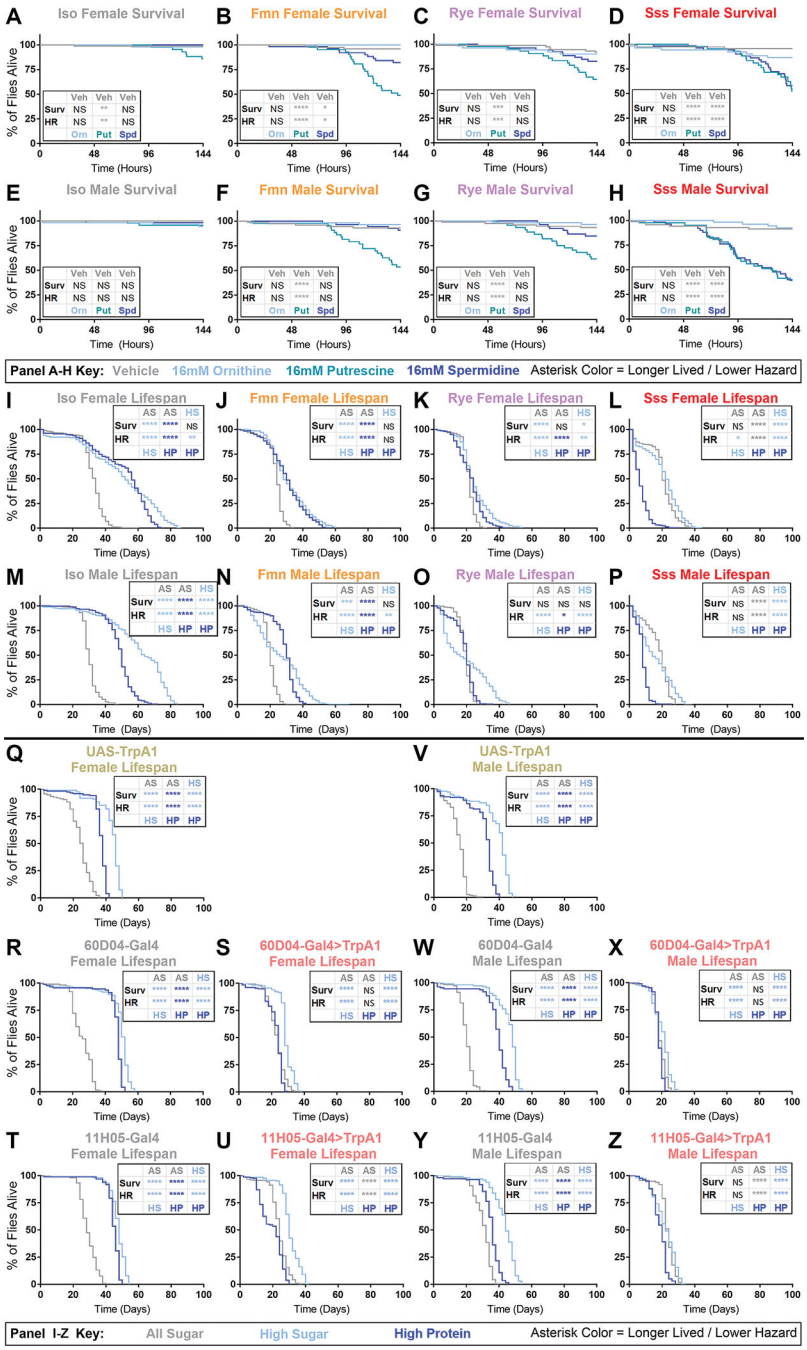

Figure 4. Dietary nitrogen is disproportionately toxic to chronically sleep-restricted *Drosophila*.

(A-H) Acute survival of female (A-D) and male (E-H) flies during exposure to water vehicle (gray), 16mM ornithine (light blue), 16mM putrescine (turquoise), or 16mM spermidine (dark blue) supplemented sugar-agar in locomotor tubes. Genotypes are *iso31* (A,E), *fmn* (B,F), *rye* (C,G), and *sss* (D,H). n=41–72 flies per group; panels show percentage survival over time of whole population, censoring flies surviving >6 days.

(I-P) Lifespan of female (I-L) and male (M-P) flies of *iso31* (I,M), *fmn* (J,N), *rye* (K,O), and *sss* (L,P) genotype. Dark blue codes high-protein diet, light blue codes high-sugar diet,

and gray codes all-sugar diet. Panels show surviving flies as a percentage of total population: n=206–239 flies per group.

(Q-Z) Lifespan of female (Q-U) and male (V-Z) flies of trpA1 control (Q,V), gal4 control (R,T,W,Y) and chronically sleep restricted gal4>trpA1 (S,U,X,Z) genotypes. Dark blue codes high-protein diet, light blue codes high-sugar diet, and gray codes all-sugar diet. Panels show surviving flies as a percentage of total population: n=93–162 flies per group; For all panels, asterisk color codes which group in each comparison had longer lifespan by Wilcoxon analysis (Surv) or lower hazard by likelihood tests of Cox proportional hazard ratios (HR). Bonferroni-corrected significance threshold for all panels is p=0.0167. *p<0.0167, **p<0.01, ***p<0.001, ****p<0.0001, NS=not significant.

Related to Figure S4 and Data S3.

KEY RESOURCES TABLE

REAGENT or RESOURCE	SOURCE	IDENTIFIER
Antibodies		
n/a		
Bacterial and virus strains		
n/a		
Biological samples		
n/a		
Chemicals, peptides, and recombinant proteins		
FCF Brilliant Blue Dye (FD&C blue no1 dye)	Spectrum Chemicals	FD110
Agar, Drosophila Type	Fisher	NC1429200
Corn Meal	LabScientific Inc	FLY-8010-20
Molasses	Gennessee Scientific	62-118
Drosophila Dry Active Yeast	LabScientific Inc	FLY-8040-10
D-Sucrose	Fisher Scientific	BP220-212
L-Ornithine Monohydrochloride	Sigma-Aldrich	O2375
Putrescine Dihydrochloride	Sigma-Aldrich	P7505
Spermidine Trihydrochloride	Sigma-Aldrich	S2501
SYBR Green PCR Master Mix	Lifetech	4364344
Mifepristone (RU486)	Sigma-Aldrich	M8046
Critical commercial assays		
Ammonia Assay Kit	Sigma-Aldrich	MAK310
Uric Acid (Urate) Assay Kit	Sigma-Aldrich	MAK077
BCA Protein Assay Kit	Abcam	ab207003
Deposited data		
HD4 unbiased global metabolomics dataset from sleep mutant and control fly heads	Metabolon	Deposited on Metabolights as MTBLS3318
Experimental models: Cell lines		
n/a		

REAGENT or RESOURCE	SOURCE	IDENTIFIER
Experimental models: Organisms/strains		
iso31 control strain	lab generated allele	PMID: 15238529 [63]
fumin (*fmn*: backcrossed 5X to *iso31*)	gift from Kazuhiko Kume	PMID: 16093388 [4]
redeye (*rye*: backcrossed 5X to *iso31*)	lab generated allele	PMID: 24497543 [5]
sleepless P1 (*sss*: backcrossed 5X to iso31)	lab generated allele	PMID: 18635795 [6]
60D04-gal4	gift from Kyunghee Koh; also available from Bloomington Drosophila Stock Center	Bloomington #45356 [15,16,64]
11H05-gal4	gift from Kyunghee Koh; also available from Bloomington Drosophila Stock Center	Bloomington #45016 [15,16,64]
UAS-trpA1 (II) (backcrossed 5X to *iso31*)	gift from Leslie Griffiths	PMID: 18548007 [65]
actin-geneswitch (actinGS: backcrossed 5X to *iso31*)	gift from Ken Irvine	PMID: 16269336 [66]
UAS-dicer2 (II) (w1118)	Vienna Drosophila Resource Center	VDRC #60008
nsyb-geneswitch (nsybGS: backcrossed 5X to *iso31*)	lab generated allele	PMID: 29590612 [67]
assorted RNAi's and sgRNA's (stock center backgrounds)	see Data S2	see Data S2
Oligonucleotides		
Drosophila asl forward qPCR primer (TCGACAAGCTGTCCCAAGTG)	Integrated DNA Technologies (IDT)	n/a
Drosophila asl reverse qPCR primer (CACCAGATAGTAGGCCCAGTC)	Integrated DNA Technologies (IDT)	n/a
Drosophila spds forward qPCR primer (GAAACACGCGCTGAAGGATG)	Integrated DNA Technologies (IDT)	n/a
Drosophila spds reverse qPCR primer (GGCATAGGCCACCTTAGCAA)	Integrated DNA Technologies (IDT)	n/a
Drosophila sms forward qPCR primer (GAGCTGCAGAACATTGCTGA)	Integrated DNA Technologies (IDT)	n/a
Drosophila sms reverse qPCR primer (GTACAACAAGGCGCCATCAC)	Integrated DNA Technologies (IDT)	n/a
Drosophila α-tub forward qPCR primer (CGTCTGGACCACAAGTTCGA)	Integrated DNA Technologies (IDT)	n/a
Drosophila α-tub reverse qPCR primer (CCTCCATACCCTCACCAACGT)	Integrated DNA Technologies (IDT)	n/a
Recombinant DNA		
n/a		
Software and algorithms		
JMP 13	JMP	Download at JMP.com
GraphPad Prism	GraphPad	Download at GraphPad.com
DAMfilescan	Trikinetics	Free download at https://trikinetics.com
Matlab	Mathworks	Download at Mathworks.com
Other		

REAGENT or RESOURCE	SOURCE	IDENTIFIER
Single-Beam Sleep Monitors	Trikinetics	DAM2
Multi-Beam (15 Beams) Sleep Monitors	Trikinetics	DAM5H